

INDUCTIVE POWER TRANSFER TOPOLOGY FOR ELECTRIC VEHICLE BATTERY CHARGING

Dr. T RAKESH

Associate Professor & HOD, Department of EEE, KLR College of Engineering and Technology, Palvoncha-507115.

Abstract—Recently, high-frequency power converter designs for restricted power transfer range inductive power transfer (IPT) systems have used power electronic converters based on zero voltage switching (ZVS) or zero current switching (ZCS). It is still difficult to use ZVS or ZCS for all power switches simultaneously in IPT systems. The improved zero-voltage zero-current trying to switch (ZVZCS) IPT architecture and its switching pattern are presented in this study. ZVS is obtained by optimising the traditional series compensation in addition to generating ZCS via an auxiliary network. MATLAB/Simulink simulations of resistive and battery load are used to verify the suggested approach. Last but not least, the outcomes using a simulink rated for 1.1 kW, 85 kHz demonstrate the realism of the suggested design. ZVZCS is capable of transferring dynamic power between 20 W and 1.1 kW with an efficiency of 91.26%.

Index Terms: electric vehicles (EVs), dc-dc power converters, wireless power transfer, inductive charging, and battery chargers.

I. INTRODUCTION

Two issues facing the expanding global economy are the depletion of fuel supply and hazardous environmental changes. Furthermore, it has spurred the creation of green technologies that have enhanced major carbon emitters such as transportation [1], [2]. Electric vehicles (EVs) are already extensively used to reduce the environmental effects of carbon-based fuels [2, 3]. Furthermore, the EV market offers a fresh opportunity for customers to prolong the life of their vehicles at a lower cost [1], [3]. Limitations in battery technology (BT) and power shaping technologies have previously hampered EV commercial performance. Nevertheless, BT has evolved over the last several decades to have a high efficiency, low weight, and high energy density [4]. Additionally, an effective energy storage device improves overall performance when used with a suitable power shaping circuit. A dc-dc power conditioning system with improved charging-discharging cycles, durability, constant energy transfer, and reduced power losses has been tested by companies and researchers [1]–[4]. For short driving distances, effective, fast chargers are being employed out of concern for human safety. Currently, inductive power transfer (IPT)-based typologies are used as safer battery charging (BC) options for EV stationary and dynamic modes. Compensation networks are provided to lower the circuit impedance and boost the converter's overall efficiency. However, the number of active and passive circuit components is connected with the setup's complexity [5].

The optimal approach improves end-user economics, driving range, maintenance cycle, and carbon footprint reduction. As a result, the converter selection is essential to the EV flow of the market. Consequently, it adeptly aids in mitigating environmental problems resulting from transportation issues [6]. One of the most often utilised network configurations by companies is the classic series-series capacitor compensation based IPT topology because of its straightforward design and operational stability over a variety of coil distances [7]. The low cost of this network compromises its efficiency, power transmission capability, high resonant peaks, and control accuracy for variation loading.

[7] offers a phase control approach to boost bandwidth efficiency, but it comes at the expense of a complicated control mechanism for a different frequency. [8] solves issues caused by variable frequency by placing the control boundary in the optimal frequency range. The control solutions covered in [7] and [8] solely serve to increase efficiency and sustain zero voltage switching (ZVS) for IPT systems. The topological advancement was made in [9] with a new coil support network that uses an intermediate L-C series compensated structure at both the transmitter and reception ends. This arrangement lowers weight

at the vehicle side by placing both coils on the primary side in [10]. However, the method given in [9] and [10], which allows magnetic flux in a misaligned scenario, detracts from the beauty of simplicity in computation and control operation. In [11], an H-bridge high-frequency transformer is combined with an L-C tank network to address the issues related to employing an isolated tank network to enable IPT. However, it increases the system's volume, weight, and size while decreasing peak efficiency. Therefore, in order to solve issues brought on by the addition of a second magnetically separated resonant tank, the network of the passive component is restored in [12]–[17]. In [12] and [13], symmetrical filter networks with loosely coupled transformer coils are cascaded to improve the system performance over a long time. However, using magnetically separated inductors in these topologies results in increased volume, weight, and tuning complexity, as well as decreased efficiency. These issues are addressed in [14] and [15] by using asymmetrical compensation while implementing the LCC-C network architecture. The LCC-LCC network is sufficient for stationary IPT and the LCC-C network is sufficient for dynamic IPT for the same coil design, according to [16] and [17], which compare the evaluations of the claims in [12] to [15].

However, when clearance and vehicle side topology change, it becomes distorted. Therefore, Zhang et al. [16] and Li et al. [17] set out to design an alternate method employing series C-C compensation. A technique for stabilising soft switching in order to improve the efficiency and performance of the strongly coupled transformer-based dc–dc converter is presented in [18]–[20]. Based on [18]–[20], the auxiliary network is used in [21] and [22] to enhance the resonant IPT topology's performance. More magnetics have been installed, which has increased continuous losses while maintaining stable operation and efficiency gains. A solution for a series C-C compensated topology based on resonant IPT is similarly presented in [23]. This viewpoint suggests that IPT with an additional circuit might assist a network powered by a voltage source inverter (VSI) fed converter in resolving a number of issues. This article suggests a topology that uses conventional series L-C compensation and small auxiliary components to combine zero current switching (ZCS) with ZVS. The recommended design maintains a steady output voltage even when the input is subjected to a wide range of voltage variations. Since the output current may be easily controlled from the input side voltage, the converter's cost is essentially reduced and a high-power CPU is not required to control operation. A laboratory prototype has been developed and tested for resistive load and battery throughout the whole BC range. The entire design, which uses modified pulsewidth modulation (MPWM) to separately control the converter's two stages, is shown in Fig. 1. In MPWM mode, the pulses are generated at a switching frequency of 85 kHz in order to achieve zero-voltage zero-current switching (ZVZCS) and provide power up to 1.1 kW. Performance information is shown.

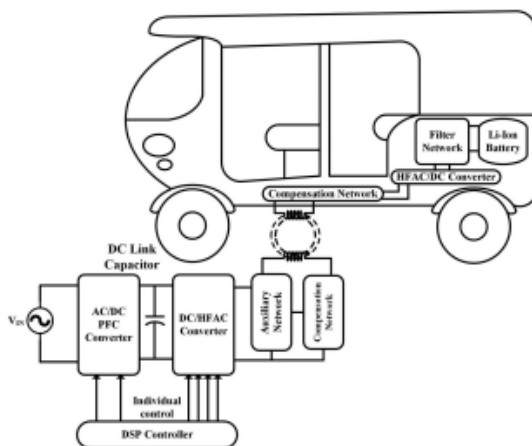


Fig. 1. General configuration of wireless battery charger topology

II. ELECTRIC VEHICLE

An electric vehicle, often known as an EV, propels itself using one or more electric motors or traction motors. An electric vehicle may be self-contained with a battery, solar panels, or an electric generator to convert gasoline to energy, or it may be fueled via a collector system by electricity from off-vehicle sources. [1] Road and rail cars, surface and underwater watercraft, electric aeroplanes, and electric spacecraft are just a few examples of EVs.

EVs first appeared in the middle of the 19th century, when electricity was one of the most popular forms of motor vehicle power. They offered a degree of comfort and convenience of use that gasoline automobiles of the day were unable to match. For over a century, modern internal combustion engines have dominated the propulsion of motor vehicles, but electric power has remained prevalent in other vehicle types, including railways and smaller vehicles of various kinds.

Due to advancements in technology and a greater emphasis on renewable energy sources, EVs had a renaissance in the twenty-first century. A small group of do-it-yourself (DIY) engineers started exchanging technical information for doing electric car conversions as there was a significant increase in demand for electric automobiles. Governmental incentives to boost adoptions have been implemented, especially in the US and the EU.



Edison and a 1914 Detroit Electricmodel 47 (courtesy of the National Museum of American History)



An EV and an antique car on display at a 1912 auto show

III. POWER FACTOR

Alternating current is virtually always used to create, transfer, and distribute electrical energy. As a result, the power factor issue is instantly raised. Since the majority of loads (such as arc lights and induction motors) are inductive in nature, their lagging power factors are often low. Because it increases current and results in increased active power losses in all components of the power system, from the generator at the power plant down to the utilisation devices, the low power factor is very unfavourable. A supply system should have a power factor that is as near to unity as feasible to provide the technical and financial circumstances that are most advantageous. We'll talk about many ways to boost power factor in this chapter.

In an a.c. circuit, power factor is the sine of the angle between voltage and current. The phase mismatch between voltage and current in an a.c. circuit is often present. Circuit power factor is referred to

by the symbol \cos . The power factor is referred to as trailing if the circuit is inductive because the current trails the voltage. Although power factor is supposed to be leading, current in a capacitive circuit leads the voltage. Think about an inductive circuit that receives a lagging current I from a supply voltage V , where the angle of lag is ϕ . In Fig. 6.1, the circuit's phasor diagram is shown.

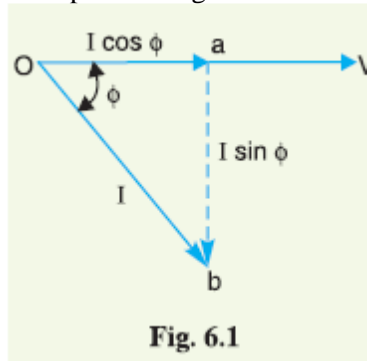


Fig. 6.1

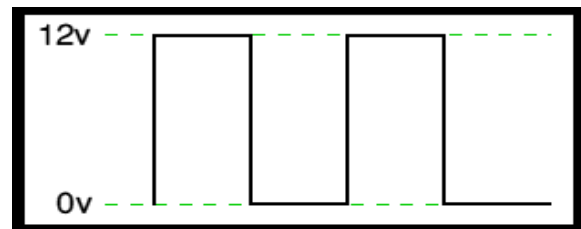
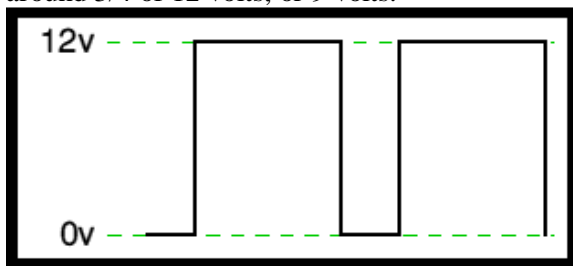
It is possible to divide the circuit current I into two perpendicular halves, namely

- (a) $I \cos$ in phase with V .
- (b) $I \sin$ 90 degrees out of phase with V .

PULSE WIDTH MODULATION

Pulse Width Modulation By switching the solar system controller's power devices, (PWM) is the most efficient way to achieve constant voltage battery charging. When using PWM control, the solar array's current tapers in accordance with the battery's state and recharge requirements. Think about the following waveform: The voltage is switched between 0 volts and 12 volts. It should be very evident that a "appropriate device" attached to its output would perceive the average voltage and believe it is being fed 6v, which is precisely half of 12v, as the voltage is at 12v for exactly as long as it is at 0v. Consequently, we may change the "average" voltage by adjusting the width of the positive pulse.

Also, if the switches maintain the voltage at 12 for three As seen below, the average voltage will be around 3/4 of 12 volts, or 9 volts.



Moreover, if the output pulse of 12 volts lasts just 25% of the whole duration, the average is

IV. PROJECT DESCRIPTION AND CONTROL DESIGN OPERATING PRINCIPLE OF THE PROPOSED CONVERTER

A H-bridge is formed of active switches $S1-S4$ on the main side and diodes $D5-D8$ on the secondary side (conventional). Additionally, to retain the soft-switching property of the circuit with BC, Ca1 and Ca2 function as potential dividers at the input with ancillary LA and TA. L1 and L2 are connected to C1 and C2 on the circuit's main and secondary sides, respectively. Using MPWM, the converter's operation is managed in [22]. To comprehend the suggested converter's functioning concept, the following presumptions are taken into account. 1) The transformer, dc source, switches, diodes, capacitors, internal switch diode, and capacitance are all excellent active and passive devices. 2) The interwinding capacitance of the transformer and the electrical series resistance of the inductor are disregarded. 3) The

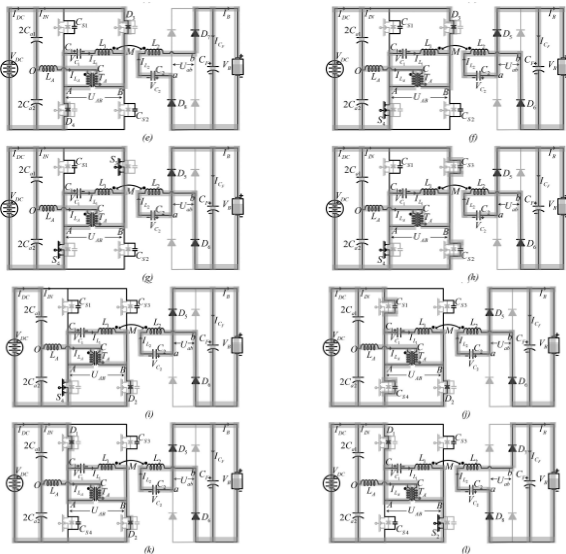


Fig. 2. Operating modes of proposed battery charger topology. (a) Mode I ($t_0 \leq t < t_1$). (b) Mode II (part-1) ($t_1 \leq t < t_{11}$). (c) Mode II (part-2) ($t_{11} \leq t < t_2$). (d) Mode III (part-1) ($t_2 \leq t < t_{21}$). (e) Mode III (part-2) ($t_{21} \leq t < t_3$). (f) Mode IV ($t_3 \leq t < t_4$). (g) Mode V ($t_4 \leq t < t_5$). (h) Mode VI (part-1) ($t_5 \leq t < t_{51}$). (i) Mode VI (part-2) ($t_{51} \leq t < t_6$). (j) Mode VII (part-1) ($t_6 \leq t < t_{61}$). (k) Mode VII (part-2) ($t_{61} \leq t < t_7$). (l) Mode VIII ($t_7 \leq t < t_8$).

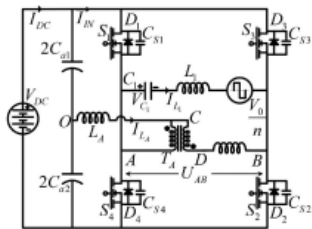


Fig. 4. Simplified network with battery load referred at transmitter coil side.

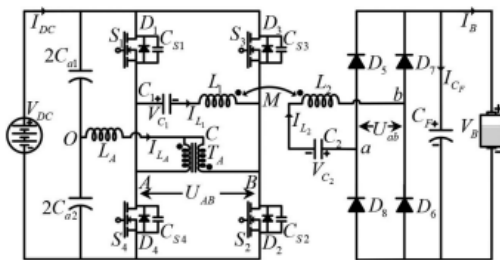


Fig. 5. Proposed network configuration of EV battery charger.

- 7) Mode VII ($t_6 \leq t < t_7$), Fig. 2(j) and (k): S4 is shut off at ZCS in this mode, and VCS4 climbs to VDC att 61. After minute 61, ILA begins to incriminate in a favourable manner. Power is sent back to the source once the diodes D1 and D2 are switched on.
- 8) Mode VIII ($t_7 \leq t < t_8$), Fig. 2(l): Transfer S2 is activated with ZVS in this mode of operation, causing current to switch from D2 to S2. Battery voltage and current are kept constant in modes I through VIII.

V. RESULTS AND DISCUSSION

By using modelling, simulation, and hardware testing, the suggested converter topology's operating principle is confirmed. To understand the behaviour of the converter, simulation and hardware circuit

settings are adjusted to an operational point. A. Results of the Simulation Principal component analysis was used in MATLAB/Simulink to simulate a suggested topology, as illustrated in Fig. 10. In Fig. 4 and Table I, ZVS turn-ON for S1–S4. The optimum DC source is connected in series with an inductor and resistor (n) (nH). To replicate the H-bridge portion of the dc-dc converter, MOSFET switches from the SimPowerSystem Library with 0 resistance and 870 pF capacitance as snubber were utilised. From mutual inductance, the linear transformer, transmitter, and reception coils contract the auxiliary transformer. As the voltage across the switch drops to zero, the gate pulse is sent to that specific switch to turn it ON. This is shown in Fig. 10 for the ZVS turn-ON of switches S1 through S4. The ZCS turn-ON for switches S2 and S4 is shown in Fig. 11(a) and (b). Before the gate pulse is finished, the switch's current drops to zero. The suggested wireless converter is hence said to maintain ZCZVS. By evaluating the performance of VC1, as seen in Fig. 12, the compensating capacitor voltage peak value is chosen. The input side characteristic of the main network is shown in Fig. 13. These findings demonstrate that the converter's performance is unaffected by the tiny value of the input dc-link capacitors. Fig. 14(a)- displays the converter's performance for BC (d). As can be seen from Fig. 14(a) and (b), there is very little disturbance. In contrast, the conventional charger causes disturbances in BC voltage and current, which shortens battery life and reduces charger efficiency. In contrast, the battery voltage and current in Fig. 14(c) and (d) are shown without the use of an auxiliary circuit. With the specifications, the circuit's performance offers 93.5 percent efficiency.

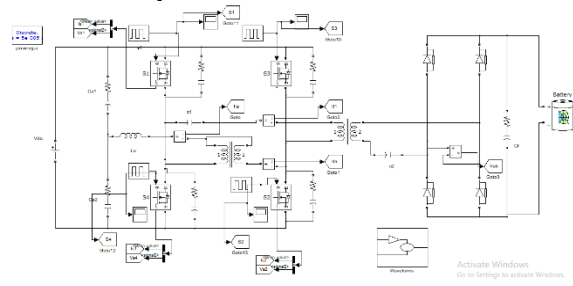


Fig: Proposed Simulation Diagram

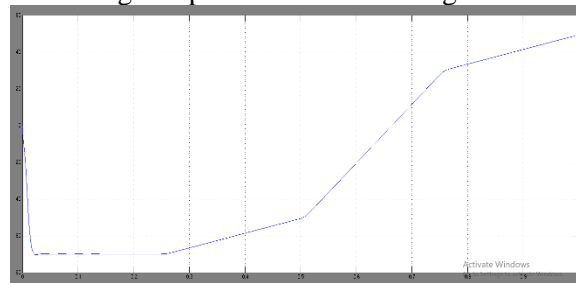


Fig: II1

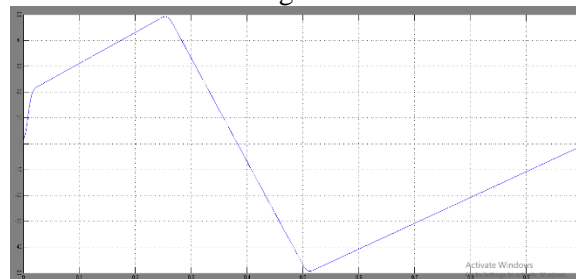


Fig: IIa

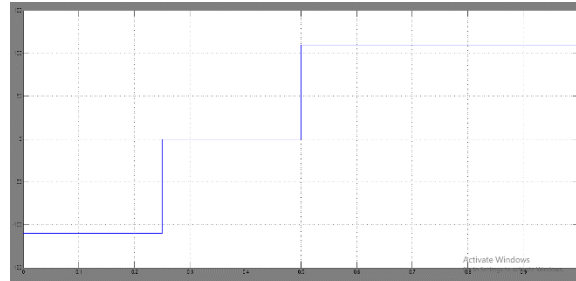


Fig: Vab

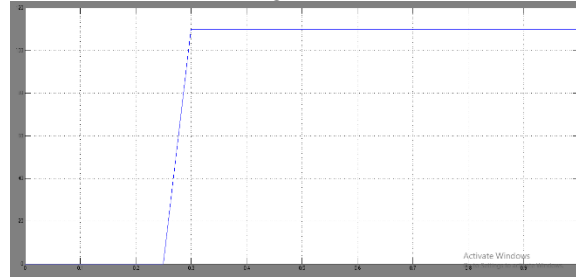


Fig: Vs1

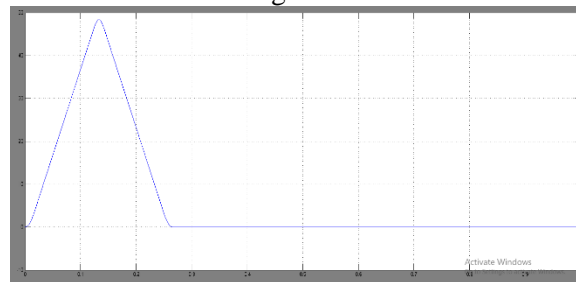


Fig: Is1

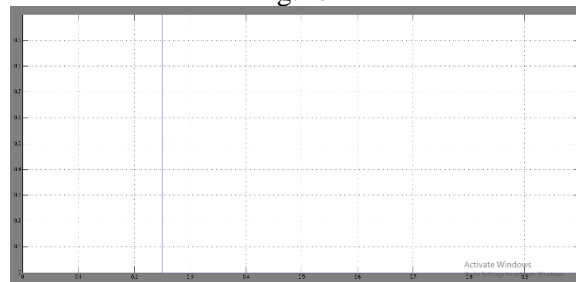


Fig: S1

VI. CONCLUSION

This article offers a tuning technique and a design for a voltage fed series compensation wireless electrical automobile battery charger. The full-bridge dc-dc converter has improved performance with a broad range of input variation because of appropriately suggested changes. When a high-power CPU is not needed, the overall cost is decreased. To get ZVZCS with less control complexity, theoretical analysis and modelling have been presented. The simulation results throughout the whole load range confirmed the ZVZCS condition of the suggested structure. The proposed technique reduced the ripple in the input/output voltage and current by utilising low values for the filter capacitance and the dc link, respectively. For resistive and battery loads, a satisfactory efficiency of 91.26 percent has been attained.

REFERENCES

[1] M. Granovskii, I. Dincer, and M. A. Rosen, "Economic and environmental comparison of conventional, hybrid, electric and hydrogen fuel cell vehicles," *J. Power Sources*, vol. 159, no. 2, pp. 1186–1193, 2006.

- [2] S. B. Peterson, J. Whitacre, and J. Apt, "The economics of using plug-in hybrid electric vehicle battery packs for grid storage," *J. Power Sources*, vol. 195, no. 8, pp. 2377–2384, 2010.
- [3] Y. Zhou, M. Wang, H. Hao, L. Johnson, and H. Wang, "Plug-in electric vehicle market penetration and incentives: A global review," *Mitigation Adaptation Strategies Global Change*, vol. 20, no. 5, pp. 777–795, 2015.
- [4] B. Nykvist and M. Nilsson, "Rapidly falling costs of battery packs for electric vehicles," *Nature Climate Change*, vol. 5, no. 4, pp. 329–332, 2015.
- [5] W. Zhang and C. C. Mi, "Compensation topologies of high-power wireless power transfer systems," *IEEE Trans. Veh. Technol.*, vol. 65, no. 6, pp. 4768–4778, Jun. 2016.
- [6] K. Mude and K. Aditya, "Comprehensive review and analysis of two-element resonant compensation topologies for wireless inductive power transfer systems," *Chin. J. Elect. Eng.*, vol. 5, no. 2, pp. 14–31, 2019.
- [7] Y. Jiang, L. Wang, Y. Wang, J. Liu, X. Li, and G. Ning, "Analysis, design, and implementation of accurate ZVS angle control for EV battery charging in wireless high-power transfer," *IEEE Trans. Ind. Electron.*, vol. 66, no. 5, pp. 4075–4085, May 2019.
- [8] Y. Jiang, L. Wang, Y. Wang, J. Liu, M. Wu, and G. Ning, "Analysis, design, and implementation of WPT system for EV's battery charging based on optimal operation frequency range," *IEEE Trans. Power Electron.*, vol. 34, no. 7, pp. 6890–6905, Jul. 2019.
- [9] D. H. Tran, V. B. Vu, and W. Choi, "Design of a high-efficiency wireless power transfer system with intermediate coils for the on-board chargers of electric vehicles," *IEEE Trans. Power Electron.*, vol. 33, no. 1, pp. 175–187, Jan. 2018.
- [10] S. Moon and G.-W. Moon, "Wireless power transfer system with an asymmetric four-coil resonator for electric vehicle battery chargers," *IEEE Trans. Power Electron.*, vol. 31, no. 10, pp. 6844–6854, Oct. 2016.